



HAL
open science

Circulation patterns in a channel reef-lagoon system, Ouano lagoon, New Caledonia

Damien Sous, Cristele Chevalier, Jean-Luc Devenon, Jean Blanchot, Marc
Pagano

► **To cite this version:**

Damien Sous, Cristele Chevalier, Jean-Luc Devenon, Jean Blanchot, Marc Pagano. Circulation patterns in a channel reef-lagoon system, Ouano lagoon, New Caledonia. *Estuarine, Coastal and Shelf Science*, 2017, 196, pp.315 - 330. 10.1016/j.ecss.2017.07.015 . hal-01566395

HAL Id: hal-01566395

<https://hal.science/hal-01566395>

Submitted on 20 Apr 2018

HAL is a multi-disciplinary open access archive for the deposit and dissemination of scientific research documents, whether they are published or not. The documents may come from teaching and research institutions in France or abroad, or from public or private research centers.

L'archive ouverte pluridisciplinaire **HAL**, est destinée au dépôt et à la diffusion de documents scientifiques de niveau recherche, publiés ou non, émanant des établissements d'enseignement et de recherche français ou étrangers, des laboratoires publics ou privés.

Circulation patterns in a channel reef-lagoon system, Ouano lagoon, New Caledonia

Damien Sous ^(a,b), Cristele Chevalier ^(b,a), Jean-Luc Devenon ^(b,a), Jean Blanchot ^(b,a), Marc Pagano ^(b,a)

^(a) *Université de Toulon, CNRS/INSU, IRD, MIO, UM 110, 83957 La Garde Cedex, France*

^(b) *Aix-Marseille Université, CNRS/INSU, IRD, MIO, UM 110, 13288 Marseille cedex, France*

Abstract

This paper reports on two three-months field experiments carried out in the Ouano lagoon, New Caledonia. This channel-type lagoon, exposed to meso-tides, south pacific swells and trade winds, has been monitored thanks to a network of currents profilers to understand the dynamics of the lagoon waters. Four typical circulation patterns have been identified, covering all together more than 90% of the survey period. These patterns are mainly driven by the waves and wind features. In particular, obliquely incident waves or strong winds blowing over a sufficient period are able to reverse the typical circulation pattern. The analysis of the vertical structure of the currents through passages shows the regular presence of a nearly linear vertical shear within the water column.

1. Introduction

Coral reefs are both invaluable and endangered living systems in the nearshore areas of tropical regions. They provide a unique habitat for countless species as well as a natural and efficient protection against erosion process and submersion events induced by storms or tsunamis (Fernando et al., 2005). Unfortunately, the reef colonies and all their benefits for biological and human populations are threatened by the combined effects of the increasing anthropic pressure and the climate change (sea level rise, acidification, warming, etc).

The hydrodynamical functioning of reef-lagoon systems remains a challenging task for coastal oceanographers. It is, from a physical point of view, a striking example of interacting processes over a wide spatio-temporal range but also a fundamental step for the characterization of the biogeochemical processes which finally govern the health and resilience of the ecosystema (Carassou et al., 2010; Szmant, 2002).

Reef-lagoon systems are potentially exposed to a wide set of physical forcings such as tides, waves, wind, coastal currents, rainfalls, river discharges and evaporation which affect the dynamics and the quality of lagoon waters. Density-driven currents have been observed between lagoon and ocean (Atkinson et al., 1981), but the overwhelming trend is that tides, waves and wind are, by far, the main drivers of lagoon circulation and water renewal in most configurations (Wolanski et al., 1993; Kraines et al., 1998, 1999; Tartinville and Rancher, 2000; Andréfouët et al., 2001; Kench and McLean, 2004; Angwenyi and Rydberg, 2005; Hench et al., 2008; Lowe et al., 2009; Taebi et al., 2011; Hoeke et al., 2013; Chevalier et al., 2014, 2015). The tidal cycles have a direct effect on the lagoon water : the lagoon fills during the flow and empties during the ebb, inducing the so called tidal ellipses representing periodically rotating currents. This basic scheme can be significantly complicated by the presence of complex lagoon bathymetry with multiple openings and

36 passages toward the open ocean and the neighbouring lagoons. The dynamics of the lagoon waters, the
37 mixing, exchanges and renewal processes as well as the residence time (Delhez et al., 1999; Monsen et al.,
38 2002; Delhez et al., 2014) are thus dramatically dependent on the lagoon geometry (atoll, barrier reef or
39 fringing reef) and volume and the passage cross-sections. The fluctuations of the still water level, mainly
40 due to tides, induces modifications of both lagoon volume and channels/passages sections. Furthermore,
41 they strongly affect the wave breaking process over the reef which determines in a large part, i.e. as soon
42 as waves break on the reef top, the cross-reef fluxes. This explains why lagoon circulation studies must take
43 into account the wave effect, and also justifies the great amount of research efforts spent to understand wave
44 transformation over reefs and related currents (Lowe et al., 2005; Monismith, 2007; Lugo-Fernandez et al.,
45 1998; Hearn, 1999; Gourlay and Colleter, 2005; Bonneton et al., 2007). The main physical processes during
46 the wave propagation, which are now fairly well understood, include refraction, reflection and shoaling on
47 the outside reef slope (Kraines et al., 1998; Symonds et al., 1995; Gourlay, 1996a,b; Massel and Gourlay,
48 2000), bathymetric breaking occurring generally before the reef top (Hardy and Young, 1996; Hearn and
49 Parker, 1988; Kraines et al., 1998), harmonic transfers toward infragravity (IG) waves (Pomeroy et al.,
50 2012; Van Dongeren et al., 2013) but also possibly to higher frequency (superharmonics) waves (Chevalier
51 et al., 2015; Masselink, 1998), dissipation by friction and interaction with co- or counter-current (Roberts
52 and Suhayda, 1983). The relative importance of each process during the wave propagation toward the shore
53 is controlled by the offshore wave features, the bathymetry, the mean water level and slope and the reef
54 roughness.

55 This rich literature shows that a great research effort has been engaged during the last two decades to
56 understand the bulk dynamics of reef-lagoon systems exposed to a set of time-varying, and often interacting,
57 forcings. In this context, the present study aims to present and analyse a long-term field survey of the Ouano
58 lagoon, New Caledonia. More than six months of current measurements have been performed in strategic
59 points of the system to better understand the lagoon interaction with the open ocean and the neighbouring
60 lagoons. The first section of the paper is dedicated to the presentation of the studied site and the experimental
61 setup. The second section summarizes the results in order to identify the main drivers of the lagoon dynamics
62 and the most typical circulation patterns, with a subsection devoted to the analysis of the vertical structure
63 of the currents. The third section discusses the observed mechanisms in a more general context, including
64 biogeochemical issues.

65 **2. Field site and experiments**

66 *2.1. Field site*

67 The New Caledonia archipelago hosts one of the largest reef structures worldwide, partly inscribed to
68 the UNESCO World Heritage List in 2008 (GRENZ et al., 2013). The study site is the Ouano lagoon (Fig.
69 1), located on the south-west coast. It is an approximately 30 km long, 10 km wide and 10 m deep channel-
70 type lagoon (Chevalier et al., 2015) mostly exposed to south pacific swell waves, trade winds and meso-tidal
71 fluctuations.

72 The lagoon is directly opened to ocean through two reef-openings in the north-west section of the reef
73 barrier. The southern opening is about 1 km wide and 10-20m deep (the *Isié* reef opening) while the northern
74 (the *Ouarai* reef opening) is the deepest, down to -60m and 1.5 km wide. The lagoon is connected to northern

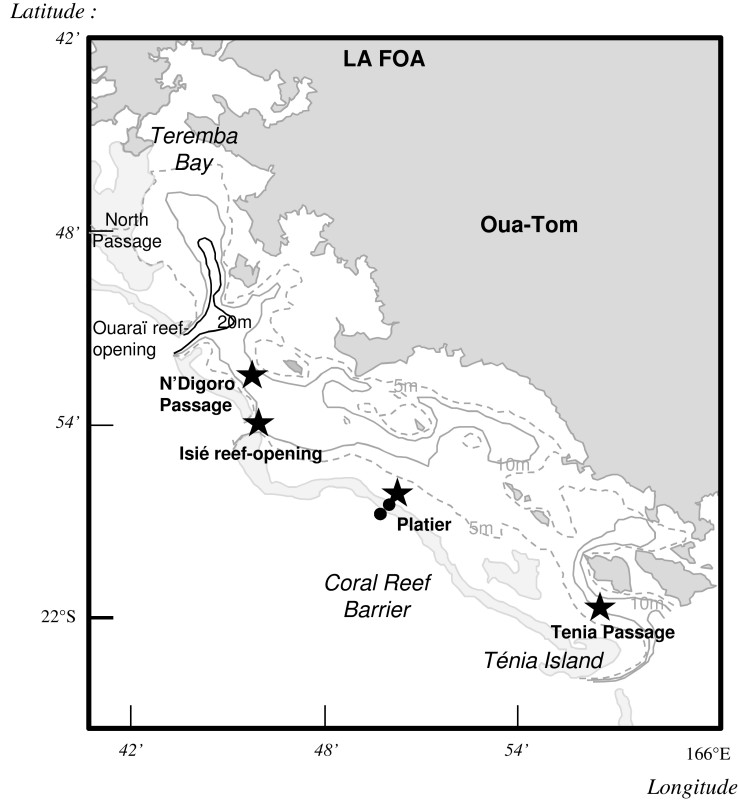


FIGURE 1: Top view of the Ouano lagoon system. Black dots and stars represent pressure sensors and velocity profilers locations, respectively.

75 and southern lagoons by two passages, one toward north and one toward south. The northern passage is
 76 about 5m deep while the south passage (the *Tenia* passage) is 10-15 m deep. Note that this latter is close
 77 to a further south reef-opening. At high tide, the coral reef barrier is fully submerged, whereas at low tide
 78 it can be partly emerged depending on tide and wave conditions.

79 In the present study, the instrumentation is focused to a well-defined lagoon system extending from the
 80 Tenia passage to the N'Digoro passage where the lagoon topography is rather simple with a limited number
 81 of openings (see Fig. 1). This simple geometry allows that the physics of the problem can be more easily
 82 understood before extending to more complex systems. In this part of the Ouano lagoon, the reef barrier
 83 is 25 km long and only opened at the Isié reef opening. The total volume of the considered portion of the
 84 lagoon is then about $1.3 \cdot 10^9 \text{ m}^3$.

85 2.2. Field experiments and methods

86 Two field campaigns have been carried out in the Ouano lagoon : the first in 2013 from August 28 to
 87 December 4 and the second in 2015, from January 10 to April 15. A first analysis of the 2013 experiment
 88 has focused on the parameterization of cross-reef fluxes in a coastal circulation numerical model (Chevalier
 89 et al., 2015). The 2013 data is here further analysed and combined with the 2015 experiment to provide a
 90 general view of the circulations patterns in the Ouano lagoon, over two different seasons including a wide

Site		Profiler Parameters						
Location	Depth	Sensor	Samp.-Aver.	Vert. res.	1st Bin	Pings/ens	Time/Ping	SD
	(m)	(min - min)	(m)	(m)			(s)	(cm/s)
2013								
N'Digoro	14.84 ±0.05	Rdi 300KHz	10-1	1.5	3.73	100	0.55	1
Isié	16.80 ±0.05	Rdi 300KHz	10-1	1.5	3.73	100	0.55	1
Platier	3.53 ±0.05	Sontek 3MHz	10-1.5	0.25	0.45	asap	nc	nc
Tenia	13.89 ±0.05	Rdi 300KHz	10-1	1.5	3.73	100	0.55	1
2015								
N'Digoro	15.71 ±0.05	Rdi 300KHz	10-1	1.5	3.73	100	0.55	1
Isié	16.19 ±0.05	Rdi 300KHz	10-1	1.5	3.73	100	0.55	1
Platier	3.31 ±0.05	Sontek 3MHz	10-1.5	0.25	0.45	asap	nc	nc
Tenia	14.20 ±0.05	Rdi 300KHz	10-1	1.5	3.73	100	0.55	1

TABLE 1: Current profilers characteristics during the field experiments (*asap* : as soon as possible - ping per ensemble, *nc* : no theoretical value calculated by Sontek).

91 range of wave, wind and tide conditions.

92 Four current profilers (ADCP) were deployed during the experiment to provide data on temporal va-
93 riability of current velocity and direction along vertical profiles. Three Acoustic Doppler Current Profilers
94 (ADCP) were deployed (Fig. 1) in lagoon passages (N'Digoro and Tenia) and reef-opening (Isié). An addition-
95 al profiler was deployed in shallower area at the onshore end of the reef flat (the *Platier* site) to measure the
96 cross-reef exchanges between lagoon and ocean. Mooring depths and profilers parameters are summarized in
97 table 1.

98 Wave dynamics on the outside reef slope was measured thanks to autonomous pressure sensors OSSI Wave
99 Gauge (5Hz sampling frequency) and RBR Duo (1Hz sampling frequency) for the first and second campaigns.
100 Pressure sensors are fixed on the bottom, at immersion depths 14.4 and 12m for the first and second expe-
101 riments, respectively. Linear theory is used to estimate free surface oscillations and related significant wave
102 height H_s from pressure measurements at the bottom over 30-min time window. Meteorological data (wind,
103 pressure and humidity) were provided by the Tontouta airport station. Offshore wave data used to relate
104 for both 2013 and 2015 campaigns the lagoon circulation with wave features, including H_s^{ww3} significant
105 wave height, T_p^{ww3} the peak period and θ^{ww3} the mean wave direction were computed by WAVEWATCH III
106 model version 4.04. In addition, statistical analysis on the wave climate have been performed on IOWAGA
107 1994-2012 numerical data (CFSR forcing).

108 Section 3.5 presents an analysis of the vertical structure of currents. A quantitative estimation of the
109 vertical shearing over the water column is provided by the calculation of the horizontal component of the
110 vorticity vector $\partial U/\partial z$. The vorticity is first calculated for each bin and then depth-averaged over the water
111 column. The vertical shear of current is generally quite linear for main velocity components at Isié, Tenia
112 and N'Digoro sites, so that the depth-averaged vorticity can be generally considered as a relevant indicator.
113 Along the reef (Platier site), the vertical structure of the current is usually much more complex which can
114 not be simply analysed in terms of depth-averaged quantities and will not be discussed here.

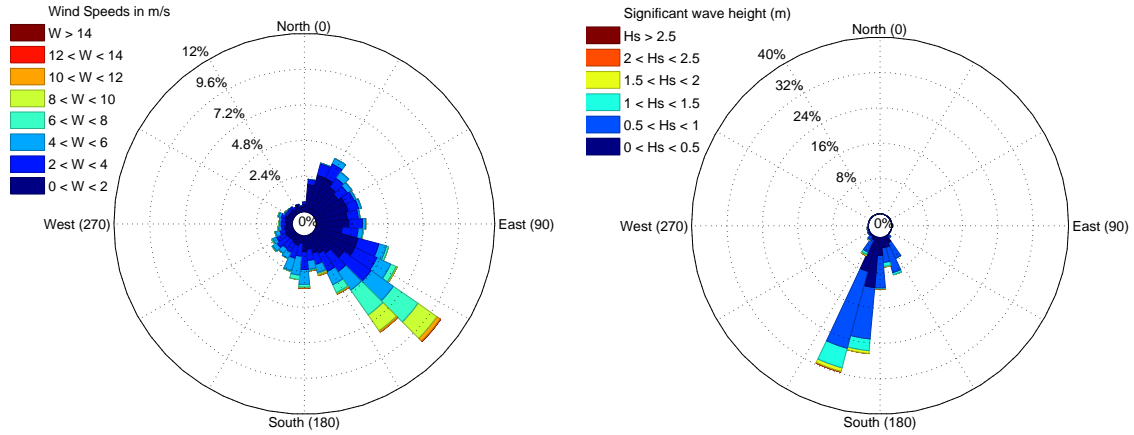


FIGURE 2: Wind rose (left) and wave rose (right) for cumulated data of both 2013 and 2015 experiments.

115 2.3. Field conditions

116 In most reef-lagoon systems, water circulation is mainly controlled by fluxes through passages, reef
 117 opening and above the immersed part of the coral barrier in response to external forcings, such as tides,
 118 waves and wind (Bonneton et al., 2007; Gourlay and Colleter, 2005; Roberts et al., 1975; Roberts and
 119 Suhayda, 1983). In the considered lagoon, the main driver is the tide, as demonstrated for instance by the
 120 spectral analysis shown in Fig 3 or the periodic oscillations of velocities observed in Figs. 4 or 5. In this
 121 paper, a particular attention is paid on the role played by the other main forcings of the lagoon system,
 122 i.e. waves and wind, through the study of five parameters : the incoming wave height H_s , peak period T_p
 123 and direction θ_{ww3} and the wind magnitude W and direction θ_w . Rainfalls have been sparse on the studied
 124 periods and are neglected.

125 Statistical features of waves and wind over the cumulated data (2013 and 2015 experiments) are sum-
 126 marized in the wind and wave roses shown in Fig 2. Wind measurements performed at the nearby Tontouta
 127 airport station revealed the typical wind pattern observed during the experiments. Trade winds are modula-
 128 ted by thermal breeze and guided by the mountainous topography of New Caledonia. The dominant pattern
 129 is clear : strong winds always blow from the south east and almost no winds are coming from the north-west
 130 sector. Daily variations are observed in Figs. 4 and 5. Winds are minimal during nights (lower than 1 m/s)
 131 and nearly offshore (north-west to north). They increase during the day while clockwise rotating and blowing
 132 from the east, then south and finally west before slowing down in late afternoon. This typical trend shows
 133 a slight seasonal variation is observed when comparing Figs. 4 and 5, the wind tends to be stronger during
 134 the spring. The mean and maximal measured values are 2.5 and 12.4 m/s for the 2013 experiment and 2.9
 135 and 12.2 for the 2015 experiments.

136 The wave distribution shown in Fig. 2, right plot, shows that waves are coming from a quite narrow sector
 137 between 140 and 215° . The main peak period is $11.7s$ which indicates the dominance of long swell waves.
 138 Mean and maximal wave heights are about 0.96 and $2.74m$ for the 2013 experiment, and 1.22 and $3.79m$ for
 139 the 2015 experiment. The strong wave events ($H_s > 1.5m$) are generally associated to direction about 200° ,
 140 with a noticeable exception around March 14, 2015 with a more south-eastern swell event.

141 3. Results

142 3.1. Overview

143 Let us first have a look on an overall directional and spectral analysis of the measured currents which
144 allows to define the variables used hereinafter. Figure 3 depicts direction probability and energy spectrum
145 for depth-averaged current at each site. As expected in the presence of strong bathymetric constraints, the
146 current are well-channelized in the reef passages and opening during the filling-emptying cycles of the lagoon
147 induced by the tide. At the Platier (reef) site, a larger directional spread is observed, but a main tendency
148 toward north is clearly observed. A more detailed analysis of current dynamics is presented hereinafter,
149 but this result allows to define, for each site, a projection axis along the main flow direction to obtain the
150 *main* and *transverse* components called U and V respectively. The sign convention is that an inward lagoon-
151 entering current is related to a positive value of the *main* component. In most cases, the analysis will be
152 performed on the main component U while the tranverse component can be neglected. The only exception
153 is the Platier site for which the transverse component $V_{platier}$ can be important.

154 The spectral analysis of depth-averaged currents presented in Fig. 3 (right plot) demonstrates the strong
155 influence of tidal components in the velocity signal : by order of decreasing importance M2 (12h25) combined
156 with S2 (12h), K1 (23h56), M4 (6h12) and M6 (4h08). As described by Chevalier et al. (2015), the amplitude
157 of water level variation shows the prevalence of the semi-diurnal and diurnal tides M2, S2 and K1 which
158 determine about 97% of the signal. To remove the influence of tides on the velocity measurements, currents
159 can be either day-averaged or detided. The former will be denoted with the superscript da in the following.
160 The latter, identified with the superscript dt , are obtained by applying band-stops filters to the current data
161 around the three dominant harmonics frequencies : $f = 2.28.10^{-5}\text{Hz}$ (M2/S2), $f = 1.16.10^{-5}\text{Hz}$ (K1) and
162 $f = 4.47.10^{-5}\text{Hz}$ (M4). As exposed in the following, day-averaged currents are the most relevant variable to
163 identify the circulation pattern at the lagoon scale while detided values will mainly be used to highlight the
164 timelag between forcings evolution and currents response.

165 One notes that the M4 component is more significant for current than for free surface spectra (dashed
166 line in Fig. 3). However, rather than a real M4 signature, this observation reveals the modulation of cross-reef
167 currents at twice the tidal frequency (Symonds et al., 1995; Kraines et al., 1998) which drives associated
168 fluctuations at other measurement sites.

169 An ensemble view of measured depth-averaged currents and main external parameters during the 2013
170 and 2015 experiments is shown in Figs. 4 and 5, respectively. The influence of tide on the depth-averaged
171 currents is strong but appears to be site-dependent, as observed on the energy spectra in Fig. 3. The tide
172 effect is clearly dominant for Isié and N'Digoro, less strong but still significant at Tenia and much smaller on
173 the reef (Platier site). In this latter location, the overwhelming trend for lagoon-entering current is related
174 to the nearly permanent wave breaking over the reef, as described by Chevalier et al. (2015). At the other
175 sites, the tide effect is much more significant, inducing intense currents alternatively inward and outward
176 during the emptying-filling cycles of the lagoon in response to tidal fluctuations. As expected, this tidal effect
177 is more pronounced at the Isié reef opening which is the only direct connection to the open ocean in the
178 considered zone. Day-averaged currents reveal that the mean general tendency is a positive (lagoon-entering)
179 current at the Platier site and a negative (lagoon-leaving) current for the three other sites. A striking feature
180 is that large wave events are associated with entering flux on the reef (Platier) and outward currents at each

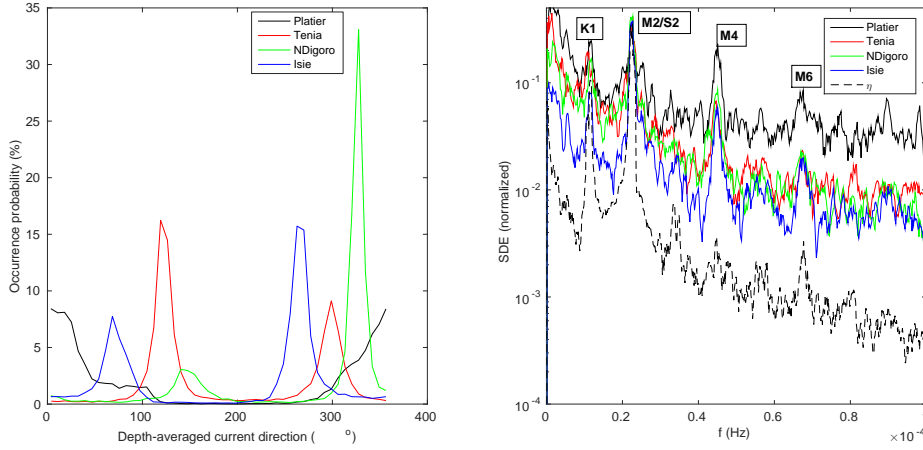


FIGURE 3: Depth-averaged current direction and normalized Spectral Density of Energy (dashed line is the SDE for the water level over the reef flat)

181 other site as shown by Chevalier et al. (2015) but this latter trend is not systematic as denoted for instance
 182 during the Feb. 8 or Mar. 14, 2015 wave events.

183 Further understanding on the lagoon dynamics is provided by the statistical inter-sites relationships
 184 depicted in Tab. 2 and in Fig. 6. Note that, for the sake of clarity, all relationships between sites are not
 185 plotted in Fig. 6 but a focus is made on the most significant ones in terms of lagoon circulation. In order to
 186 withdraw the effect of tide, the analysis of the dominant trends is performed on the day-averaged currents.
 187 The effect of external parameters, waves and wind, on the measured currents is discussed later on in sections
 188 3.2 and 3.3. Further analysis will be carried throughout the text to finally characterize the circulation patterns
 189 in section 3.4.

190 The following trends on links between sites can be deduced from Tab. 2 and Fig. 6.

- 191 — Strong connection is observed between the two northern sites N'Digoro and Isié. The day-averaged
 192 currents are generally negative (outward) and nearly linearly related (black circles in Fig. 6 A).
- 193 — The correlation is weaker between northern and southern passages (see U_{tenia}^{da} and $U_{ndigoro}^{da}$ in Fig. 6
 194 A). One notes that strong currents at Tenia can be either in- or outward while weak northern flow
 195 conditions are associated to outflow in Tenia.
- 196 — The Platier main component is fairly anti-correlated to the N'Digoro site. A similar link, not shown
 197 here, is observed with Isié.
- 198 — A strong connection is observed between U_{tenia}^{da} and $V_{platier}^{da}$. However, slightly different slopes in
 199 the $U_{tenia}^{da}/V_{platier}^{da}$ relationships are observed for positive and negative currents (see dash-dotted and
 200 dashed lines in Fig. 6, B). As discussed later on in section 3.4, this latter trend tends to indicate two
 201 distincts functionings of the southern part of the lagoon : south-eastward currents should be associated
 202 to converging water fluxes in the Tenia passage leading to a magnitude increase of U_{tenia}^{da} with respect
 203 to $V_{platier}^{da}$ while, on the opposite, periods of north-westward velocities correspond to more defined
 204 (channelized) current entering the lagoon through Tenia and flowing along the reef barrier allowing a
 205 better flux conservation between both sites.
- 206 — The linear correlation between day-averaged U_{tenia}^{da} and $V_{platier}^{da}$ is very weak. However, Fig. 6, B,

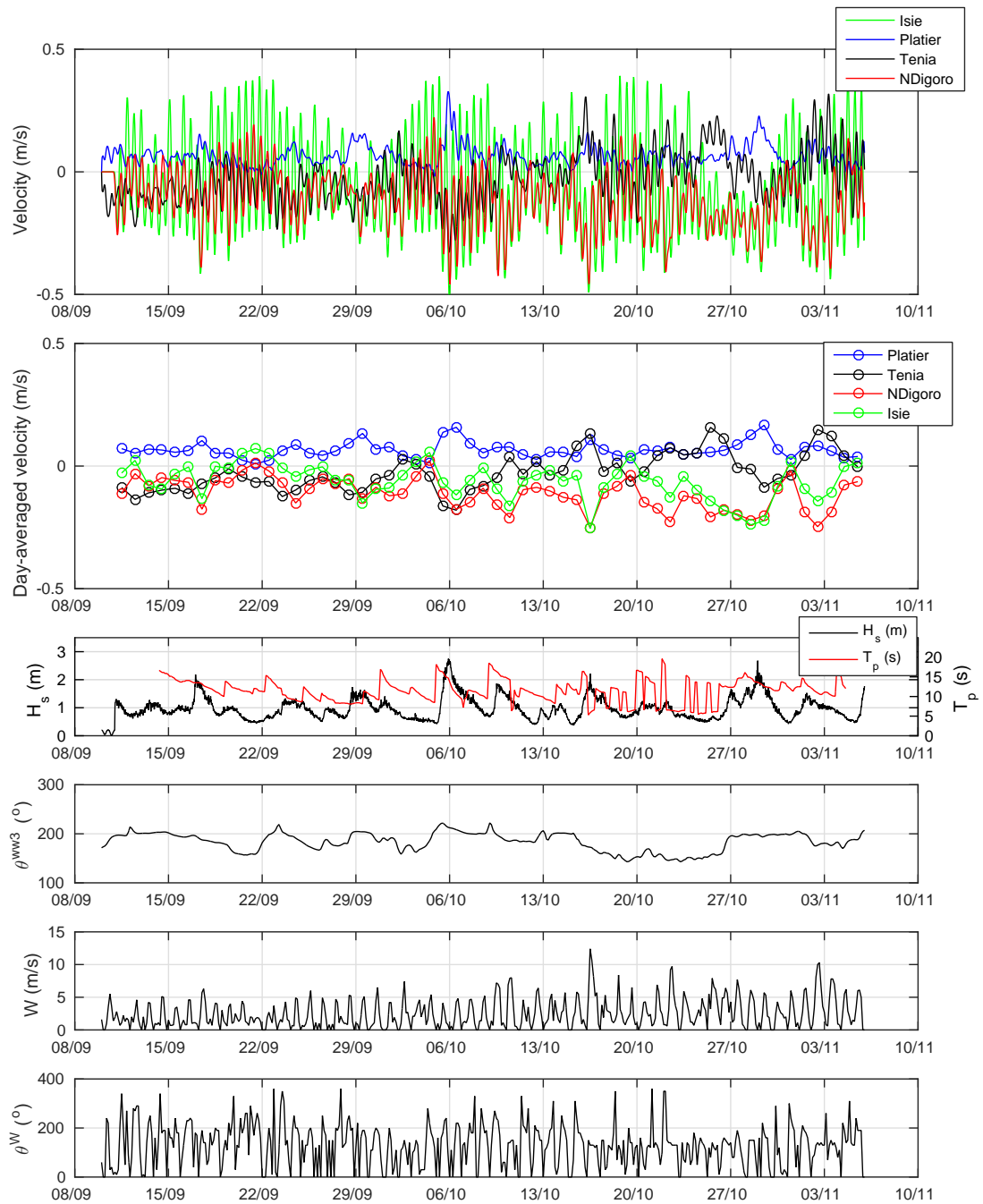


FIGURE 4: Data overview for the 2013 experiment. From top to bottom : depth-averaged currents, detided depth-averaged currents, significant wave height and peak period at the reef outer slope sensor, wave direction from WW3, wind intensity and direction.

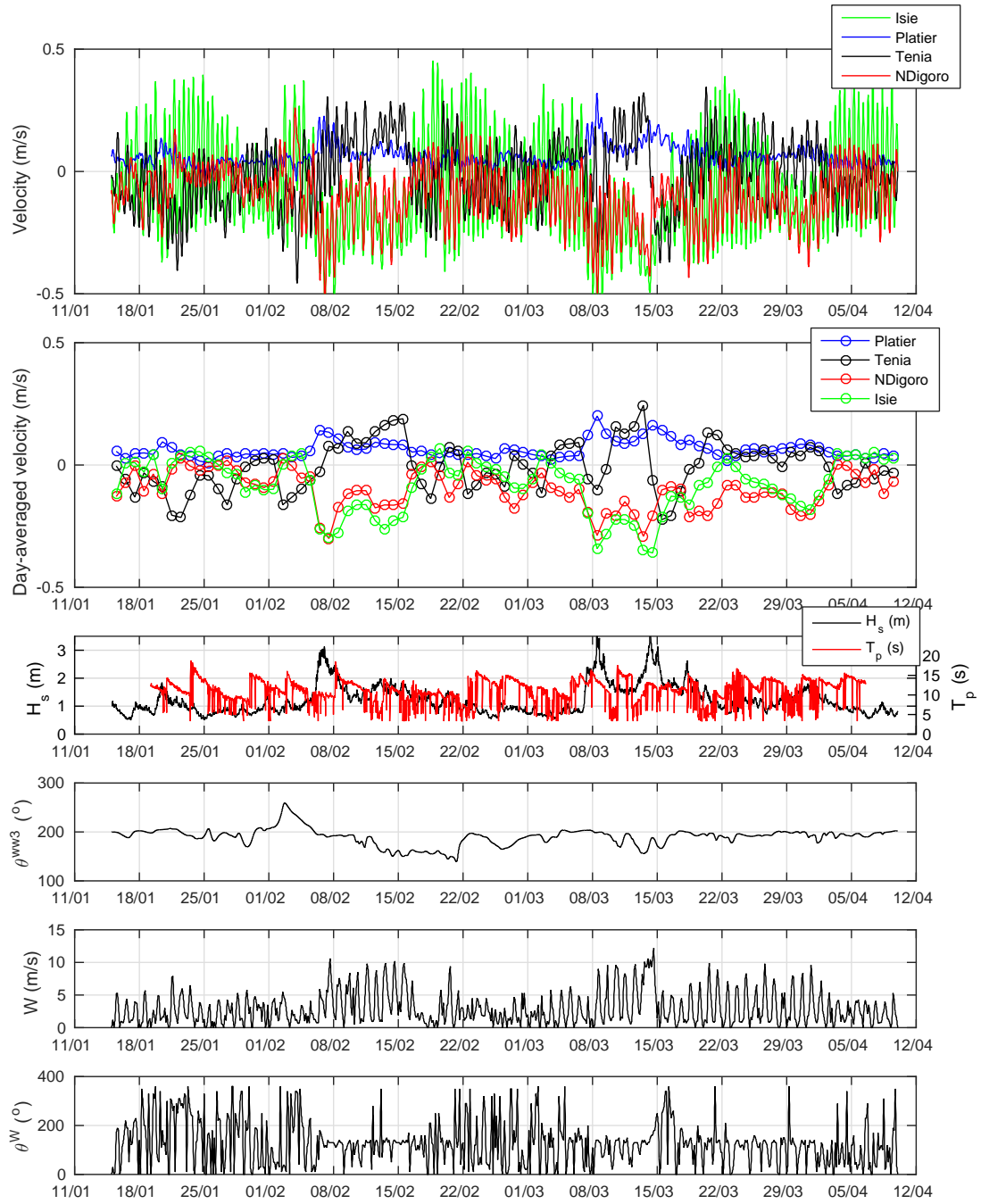


FIGURE 5: Data overview for the 2015 experiment. From top to bottom : depth-averaged currents, detided depth-averaged currents, significant wave height and peak period at the reef outer slope sensor, wave direction from WW3, wind intensity and direction.

	U_{isie}	$U_{ndigoro}$	$U_{platier}$	U_{tenia}	$V_{platier}$	U_{isie}^{da}	$U_{ndigoro}^{da}$	$U_{platier}^{da}$	U_{tenia}^{da}	$V_{platier}^{da}$
U_{isie}	-	73.4	-31.3	12.1	-40.6	-	-	-	-	-
$U_{ndigoro}$	-	-	-38.3	-14.6	-41.4	-	-	-	-	-
$U_{platier}$	-	-	-	6.3	9.7	-	-	-	-	-
U_{tenia}	-	-	-	-	54.5	-	-	-	-	-
U_{isie}^{da}	-	-	-	-	-	-	81.5	-81.5	-44.2	-37.7
$U_{ndigoro}^{da}$	-	-	-	-	-	-	-	-71.3	-56.1	-49.1
$U_{platier}^{da}$	-	-	-	-	-	-	-	-	-1.3	-0.3
U_{tenia}^{da}	-	-	-	-	-	-	-	-	-	89.3
H_s	-33.5	-41.9	77.6	-4.3	-4	-77.5	-66.5	94.5	-4.6	-6.9
T_p	-3.9	-1.7	14.4	-12.2	-11	-11.8	-8.4	23.8	-14.4	-15.2
θ^{ww3}	10.3	6.7	5.2	-30.1	-26.7	10.1	15.2	6.8	-40.9	-38.5
W	-14.1	-15.9	7.9	20.4	8.9	-63.7	-58.2	40.3	60.1	59.9
θ^W	3.9	5.2	-3.2	-10.4	-10.7	20.5	21.3	-4.8	-31.7	-29.2

TABLE 2: Correlation coefficients (in %) quantifying the currents dependence to external forcings and the inter-relationships

207 shows that : (i) $U_{platier}^{da}$ is systematically positive, (ii) the strongest values of $U_{platier}^{da}$ are associated to
208 negative U_{tenia}^{da} and, (iii), for moderate Platier currents, currents through Tenia passage can be either
209 in- or outward.

210 Correlation coefficients for complete velocity signals presented in Tab. 2 are generally much lower than
211 their day-averaged counterparts. This highlights in particular the role of phase shift during the tide pro-
212 pagation inside the lagoon : the tidal filling-emptying cycles are not in phase at each site, as described by
213 Chevalier et al. (2015).

214 3.2. Wave effect

215 Table 2 shows that, as expected, the influence of waves and wind is greater on the day-averaged currents
216 as the tidal-related components have been removed from the signal. The significant wave height H_s is, apart
217 from the tide, the dominant external parameter affecting the main current component at Isié, N'Digoro and
218 Platier sites. The sign of correlation coefficients indicates that an increase of significant wave height promotes
219 (negative) outward directed currents at Isié and N'Digoro sites and inward (positive) current over the reef at
220 Platier. This is confirmed in Fig. 7A which shows a monotonic increase of the magnitude of U_{isie}^{da} and $U_{platier}^{da}$
221 when increasing the incoming significant wave height. The overall tendency is that the increase of offshore
222 wave energy induces stronger inward cross-reef fluxes generated by wave-breaking above the barrier. This
223 water input all along the reef barrier is compensated by outward currents in each passage and reef opening,
224 see (Chevalier et al., 2015) for a parameterization of wave-induced cross-reef fluxes. The response of the

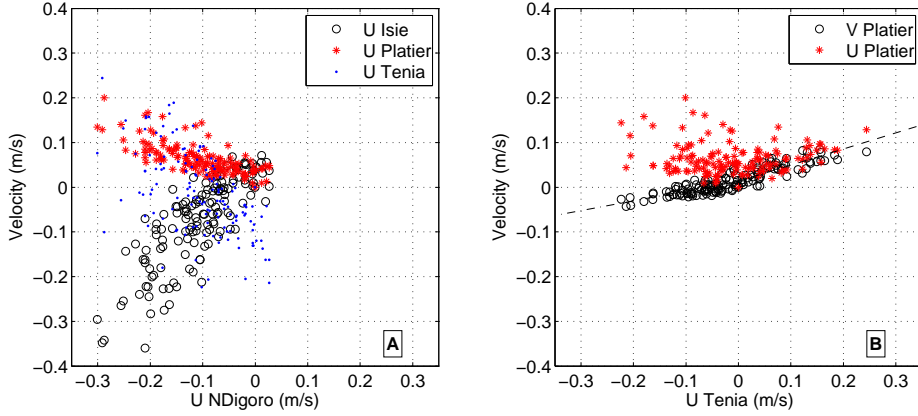


FIGURE 6: Inter-connections between day-averaged detided currents at selected sites. A : U_{isie}^{da} (black circles), $U_{platier}^{da}$ (red stars) and U_{tenia}^{da} (blue dots) vs U_{tenia}^{da} . B : $V_{platier}^{da}$ (black circles) and $U_{platier}^{da}$ (red stars) vs U_{tenia}^{da} . Dash-dotted and dashed lines are linear regression for $V_{platier}^{da}$ vs U_{tenia}^{da} for negative and positive values of U_{tenia}^{da} , respectively.

225 N'Digoro currents (not depicted here) is very close to the Isié one. However, this general circulation trend,
 226 already depicted in Chevalier et al. (2015), is not the sole circulation system in the lagoon. In particular, at
 227 Tenia (see blue dots in Fig. 7A), the day-averaged currents show no clear correlation with wave height and
 228 most of wave conditions are possibly associated to inward or outward currents.

229 The question arises now on the external conditions controlling the flushing or filling dynamics through the
 230 Tenia passage. While wave period does not show any noticeable statistical effect on depth-averaged currents,
 231 wave direction tends to anti-correlated with day-averaged U_{tenia}^{da} and $V_{platier}^{da}$ with moderate correlation
 232 coefficients being -40.9 and -38.5 % respectively. Fig. 7B depicts the corresponding relationships. In spite
 233 of the measurement spread, one notes the overall trend that eastern wave direction tend to promote positive
 234 current in Tenia and along the reef at Platier while western swells induce outflow at Tenia.

235 3.3. Wind effect

236 The correlation coefficients on both complete and day-averaged currents are presented in Fig. 8. The
 237 statistical effect of wind on the day-averaged lagoon dynamics is noticeable. It is negatively correlated with
 238 the northern sites and positively correlated anywhere else : strong south-east winds promote a north-west
 239 bulk motion within the lagoon ($V_{platier} > 0$) and throughout the reef passages ($U_{tenia} > 0$ and $U_{ndigoro} < 0$)
 240 and openings ($U_{isie} < 0$). In addition, additional computations have shown that the wind effect is quite
 241 weaker when using detided currents : correlation coefficients are -30.3, -23.8, 17.5, 28.2 and 25.3% for U_{isie}^{dt} ,
 242 $U_{ndigoro}^{dt}$, $U_{platier}^{dt}$, U_{tenia}^{dt} and $V_{platier}^{da}$, respectively. This trend is confirmed in Fig. 8 which depicts the wind
 243 correlation with detided and day-averaged transverse along-reef Platier current. The observed difference
 244 between subplots demonstrates the inertia of the lagoon waters with respect to the wind forcing. The poor
 245 correlations between wind and detided currents (or even more with instantaneous currents as presented in
 246 Tab. 2) show that the lagoon currents do not directly react to the thermal breeze cyclic rotations of the
 247 tradewinds but at a longer time scale which is better revealed by day-averaged current values. The negative
 248 detided currents observed in Fig. 8 (left) during stron winds conditions precisely correspond to the slow and
 249 delayed ajustement of the lagoon circulation to wind forcing. Fig. 8 also shows the presence of a threshold

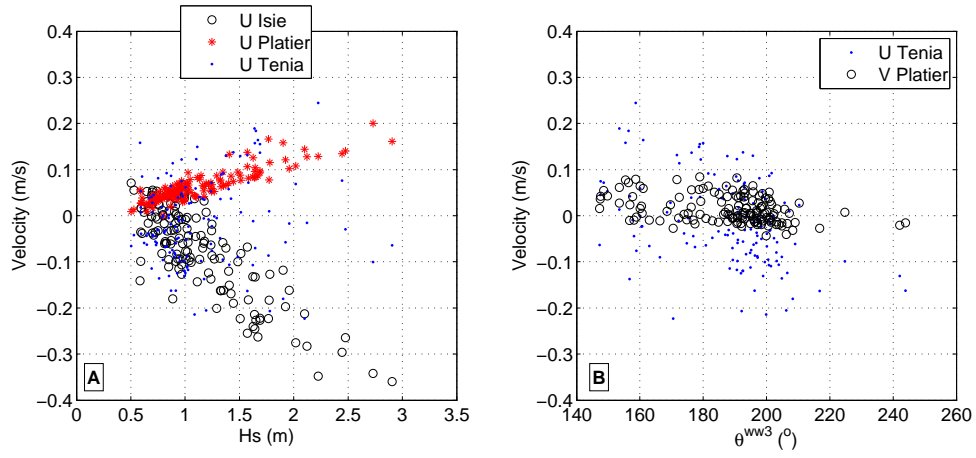


FIGURE 7: Influence of incoming wave features on the depth-averaged currents at selected sites. A : U_{isie}^{da} (black circles), $U_{platier}^{da}$ (red stars) and U_{tenia}^{da} (blue dots) vs H_s . B : U_{tenia}^{da} (blue dots) and $U_{platier}^{da}$ (black circles) vs θ^{ww3} .

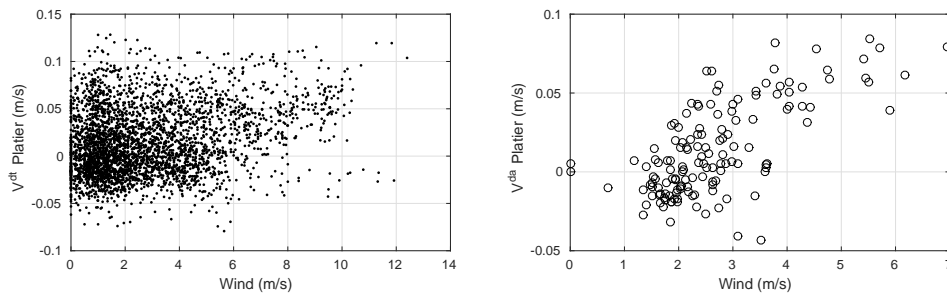


FIGURE 8: Influence of wind features on the depth-averaged along-reef current at Platier. Left : detided current. Right day-averaged current.

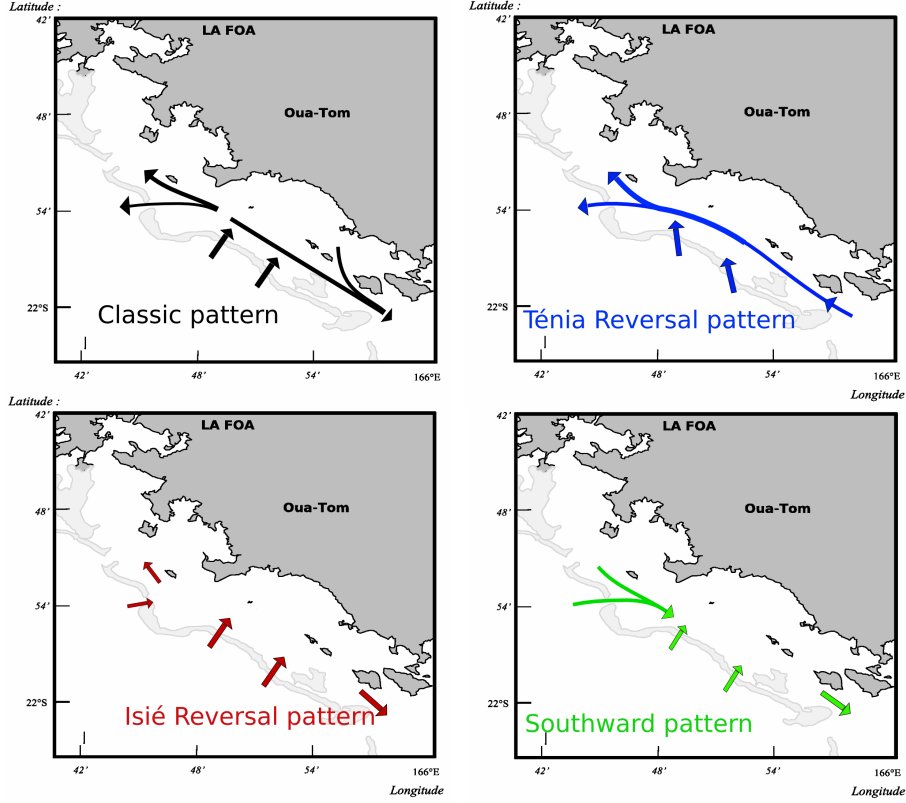


FIGURE 9: Schematic view of the circulation patterns in the Ouano lagoon.

250 in wind intensity around 3m/s from which $V_{platier}^{da}$ increases with wind intensity. For wind speed greater
 251 than 4m/s, $V_{platier}^{da}$ is systematically positive. As observed in the wind rose in Fig. 2, such strong winds are
 252 coming from a narrow directional band between 125 and 140° (in nautical convention). Similar tendencies
 253 with same wind intensity thresholds are observed at Tenia, Isié and N'Digoro sites.

254 3.4. Circulation patterns

255 The careful consideration of the presented data leads us to identify four dominant circulation patterns in
 256 the Ouano lagoon : the Classic Pattern (CP), the Tenia Reversal Pattern (TRP), the Isié Reversal Pattern
 257 (IRP) and the Southward Pattern (SP).

258 The hydrodynamical features (Fig. 9), occurrence probabilities (Tab. 3) and onset conditions (Fig. 10)
 259 for each pattern are described below. The two dominant ones, i.e. CP and TRP, are described in more
 260 details through two four days selected events in Fig. 11. Furthermore, in order to understand their role in
 261 the lagoon flushing dynamics, one representative 24h-period has been selected for each pattern among the
 262 dataset : Sept. 21 2013 for SP, Sept. 22 2013 for IRP, Oct. 6 2013 for CP and Feb. 7 2015 for TRP. The
 263 measured depth-averaged currents are thus time-averaged over the corresponding 24h period and displayed
 264 in Tab. 4. Estimation of related exchanged daily fluxes can be computed by using the cross-section areas of
 265 each site provided by the numerical bathymetry used by Chevalier et al. (2015). For the N'Digoro, Isié and
 266 Tenia sites, these cross-sections are about $2.09 \cdot 10^4$, $1.15 \cdot 10^4$ and $2.85 \cdot 10^4$ m², respectively. For Platier, as the

	CP ^{da}	TRP ^{da}	IRP ^{da}	SP ^{da}
Sept. - Nov. 2013	54.4	29.8	10.5	3.5
Jan. - Apr. 2015	27.9	40.7	19.8	5.8
Total	38.5	36.4	16.1	4.9

TABLE 3: Occurrence probabilities (in %) for the four selected patterns for day-averaged (*da*) currents.

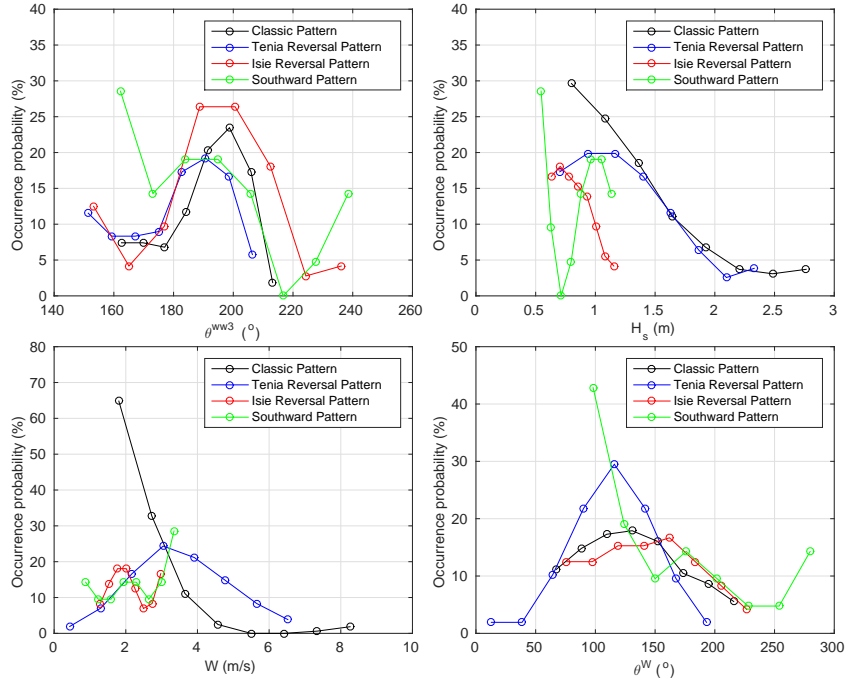


FIGURE 10: Classic and Tenia patterns

267 measurements are not performed on the top of the reef flat but on the inside slope of the barrier, the cross-
268 sectional area is estimated around the -3.5m isobath. It should be emphasized that the exchanged fluxes are
269 subject to uncertainties due to the lack of precise bathymetric survey and better spatially-resolved current
270 monitoring. They should thus be interpreted with caution and only used for inter-comparison purposes.

271 *The Classic pattern.*

272 The Classic pattern (CP) is characterized by :

- 273 — An inward flow above the reef barrier ($U_{platier} > 0$)
- 274 — An outward flow in each passage and reef opening ($U_{isie} < 0, U_{ndigoro} < 0, U_{tenia} < 0$)

275 The probability of occurrence of CP is 53.6% (Tab. 3). This is thus the dominant circulation pattern in
276 the lagoon. Figure 11 (left plots) shows a typical period of CP occurring from Oct. 5 to Oct. 8, 2013. One
277 notes first that the setting up of the current pattern is related to the arrival of a large south-west swell event
278 during the day of Oct. 5. The wave-breaking over the reef barrier induces an inward cross-reef flux at the
279 Platier site. This flux, which progressively increases with increasing wave energy, promotes lagoon-leaving
280 currents at other measurement sites. It is remarkable to note that even the flood tide at Tenia and N'Digoro

	CP	TRP	IRP	SP
H_s (m)	1.9	2.4	0.6	0.5
T_p (s)	10.7	13.2	10.8	9.2
H_s^{WW3}	2.2	1.9	0.8	0.7
T_p^{WW3}	10.7	13.5	10.9	9.1
θ^{WW3}	208	191	196	163
W (m/s)	1.9	6	1.5	1.5
θ^W	120	126	107	205
U_{isie}	-10.9	-29.1	5.8	7.9
$U_{ndigoro}$	-16.8	-29.7	-2.2	1.3
$U_{platier}$	15.5	13.2	2.4	0.9
U_{tenia}	-17.6	7.8	-6.3	-6.5
F_{isie}	-1.2	-3.3	0.7	0.9
$F_{ndigoro}$	-3.5	-6.2	-0.5	0.3
$F_{platier}$	10.2	8.7	1.6	0.6
F_{tenia}	-5	2.2	-1.8	-1.9

TABLE 4: Day-averaged currents (U in cm/s) and corresponding estimated exchanged fluxes (F in $10^3 \text{ m}^3 \cdot \text{s}^{-1}$) for four selected days corresponding to the four circulation patterns. Day-averaged values of wave and wind features are indicated for comparison.

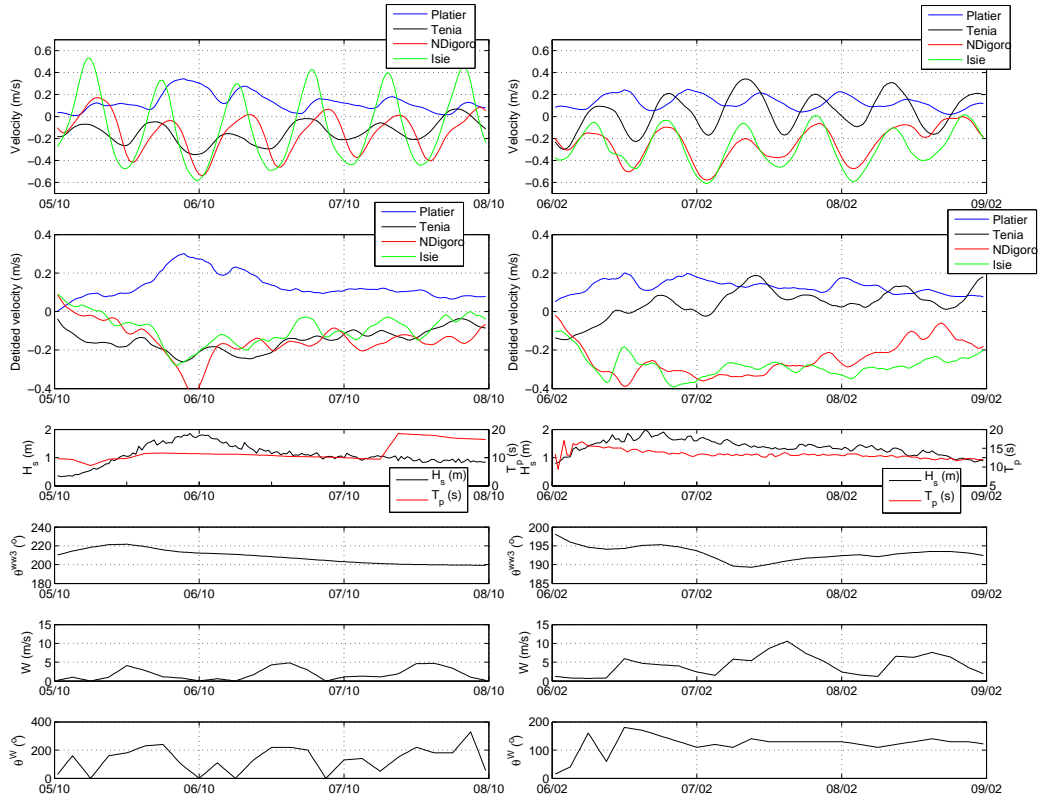


FIGURE 11: Examples of Classic Pattern and Tenia Reversal Pattern. From top to bottom : depth-averaged currents, depth-averaged detided currents, wave height and peak period, wave direction, wind intensity and direction.

281 sites is not able to compensate the outward flow. Currents are maximal around the swell apex, at high tide
 282 at Platier and during the ebb for other sites.

283 The onset conditions of CP for day-averaged currents are synthesized in Fig. 10. It is generally asso-
 284 ciated to large south-western swells and rather moderate winds. It appears that for the largest swells, CP
 285 is systematically observed, i.e. the lagoon-entering cross-reef flux is strong enough to dominate any other
 286 process. The breaking process over the reef is dependent of the ratio between wave height and water level
 287 above the reef (Hearn, 1999; Bonneton et al., 2007; Chevalier et al., 2015). When strong waves combines
 288 with low tidal amplitude, the cross-reef flux induced by wave breaking can be so important that it pushes
 289 out water through each passages and reef opening (i.e. even at Isié) all along the tidal cycles, as depicted in
 290 Fig. 4 around Sept. 29 or Oct. 31, 2013. However, more data in large wave conditions ($H_s > 3m$) should be
 291 gathered to substantiate this observation.

292 Day-averaged currents and estimated fluxes are given in Tab. 4 for the October, 6. One notes that, if
 293 depth-averaged velocities are of the same order of magnitude for each site, the input flux over the reef barrier
 294 is much more important than through passages and reef openings. Furthermore, the outward flux in Tenia is
 295 2.5 times the along-reef flux in Platier, indicating the convergence process in the southern part of the lagoon.

296 *The Tenia reversal pattern.*

297 The Tenia reversal pattern (TRP) is characterized by :

- 298 — An inward flow above the reef barrier ($U_{platier} > 0$)
- 299 — An inward flow through Tenia passage ($U_{tenia} < 0$) generally associated to north-west current along
- 300 the reef ($V_{platier} > 0$).
- 301 — An outward flow in the northern sites ($U_{isie} < 0, U_{ndigoro} < 0$)

302 The occurrence probabilities of TRP for day-averaged currents are 28.6 %, respectively. A typical TRP is
 303 depicted in Fig. 11 (right plots) between Feb. 6 to 9, 2015. The main difference with CP is the observation
 304 of an inward flow at Tenia which magnitude oscillates with the tide but can remain in the same direction
 305 during several tidal cycles. The cross-reef flux measured at Platier site is still positive but a bit less intense
 306 during the swell peak than in CP presented above for similar type of wave height. This is attributed to the
 307 combined effects of, (i), a more southern wave direction which induces more westward (indeed WNW) flow
 308 above and along the reef and, (ii), a stronger south-east wind which drives lagoon waters toward north-west.
 309 However, in the considered case, the wind peak occurs after the establishment of the pattern. This latter
 310 appears thus to be mainly initiated by the swell arrival. TRP is related to a bulk north-west motion along the
 311 barrier (see the relationship between U_{tenia} and $V_{platier}$ in Fig. 6, B), with water entering through Tenia from
 312 the neighbouring south-east lagoon and above the reef-barrier pushed by wave-breaking of south/south-east
 313 swell and leaving the lagoon through the northern openings.

314 Figure 10 shows that TRP is promoted by south to south-east swells and strong winds which are generally
 315 from south-east (Fig. 2). The comparison of estimated fluxes in Tab. 4 shows that, for similar range of
 316 incoming wave height, the exchanged fluxes through Isié and N'Digoro are much stronger in the TRP case.
 317 This emphasizes the major role played by the circulation patterns, driven by wave direction and wind
 318 magnitude, on the lagoon flushing dynamics and water renewal (Chevalier et al., 2014).

319 ***The Isié reversal and Southward patterns.***

320 The Isié reversal and Southward patterns are discussed conjointly because they occur in quite similar
 321 conditions, i.e. small to moderate waves (typically $H_s < 1.2\text{m}$) and weak winds (typically $W < 4\text{m/s}$) as
 322 depicted in Figs. 4 and 10. These patterns are not very stable and small waves periods are often characterized
 323 by alternating periods of IRP and SP.

324 Both Isié Reversal Pattern (IRP) and Southward Pattern (SP) are characterized by :

- 325 — An inward flow above the reef barrier ($U_{platier} > 0$)
- 326 — An inward flow through Isié reef opening ($U_{isie} > 0$)
- 327 — An outward flow in Tenia ($U_{tenia} < 0$)

328 The only difference is that N'Digoro current is inward ($U_{ndigoro} < 0$) for SP and outward ($U_{ndigoro} > 0$) for
 329 IRP. The occurrence probabilities for IRP and SP are respectively 12.5 and 3.6 % in terms of day-averaged
 330 currents. The estimation of exchanged fluxes in Tab. 4 for selected 24h period of IRP and SP indicates that
 331 these patterns, associated to low wave energy, are much less effective in the advection of water mass.

332 *3.5. Vertical structure*

333 The vertical structure of lagoon currents and its effect on the lagoon hydrodynamics, water renewal and
 334 biogeochemical processes have been little studied to date. Strong vertical variability has been highlighted in
 335 the Majuro Atoll numerical model (Kraines et al., 1999), with fast wind-driven surface layer (down to few
 336 meters) and much weaker or even return flows deeper in the water column possibly affected by baroclinic
 337 effects. The present data is purely hydrodynamical, i.e. the water properties such as salinity or temperature,

338 which play a dominant role in stratification processes, are not documented by measurements. However,
339 limiting our discussion to a purely currentological analysis, interesting observation can be performed on the
340 vertical structure of flows through passages and reef openings.

341 As described in Section 2.1, the depth-averaged horizontal component of the vorticity $\frac{\partial U}{\partial z}$ is computed to
342 provide a quantitative estimation of the vertical shear. Fig. 12 shows the relationship between depth-averaged
343 vorticity and main component of currents for each site. Color levels in left and right columns indicate wind
344 magnitude and wave height, respectively. Only one third of the dataset are depicted for the sake of clarity.
345 These plots should be interpreted as follows :

- 346 — Zero vorticity : no vertical shear in the water column.
- 347 — Both positive vorticity and velocity : the current over the whole water column is entering into the
348 lagoon, the surface layer moves faster than the bottom water.
- 349 — Both negative vorticity and velocity : the current over the whole water column is leaving the lagoon,
350 the surface layer moves faster than the bottom water.
- 351 — Positive vorticity and negative velocity : the depth-averaged current leaves the lagoon, the bottom
352 layer moves faster than the surface layer. In some cases, this latter can even flows in an opposite
353 direction (i.e. being positive lagoon-entering) than the bottom layer.
- 354 — Negative vorticity and positive velocity : the depth-averaged current enters the lagoon, the bottom
355 layer moves faster than the surface layer. In some cases, this latter can even flows in an opposite
356 direction (i.e. being negative lagoon-leaving) than the bottom layer.

357 One notes first, for a substantial portion of the measured data, the importance of the vertical shear. For
358 illustration, a vertical vorticity of 0.05 s^{-1} over a 10m deep measurement water column leads to a vertical
359 variation of the velocity of 0.5m/s. The presence of flow reversal within the water column, i.e. opposite
360 directions for surface and bottom layers, is observed in 16, 28, 29 % of the considered data for the Isié, Tenia
361 and N'Digoro sites, respectively. It occurs generally during the tide reversal, when depth-averaged velocities
362 are small.

363 The data distribution observed in Fig. 12 shows two overall tendencies : vertical shear generally increases
364 with current velocity and vorticity is preferentially of the same sign as velocity, i.e. surface water moves
365 faster than bottom one. The main exception to this trend is observed at Isié where inward current can
366 show significant vorticity either positive or negative. In addition to this base functioning, the effects of wind
367 and wave on the vertical shear are displayed by color labels in left and right columns, respectively. Strong
368 winds (blowing from south-east) are generally associated to strong (negative) vertical shear associated with
369 the outward currents at Isié and N'Digoro. This describes the expected effect of wind which enhances the
370 north-west surface transport over the whole lagoon. At Tenia, the wind does not show a direct effect on the
371 vertical shear and strong wind events are mainly associated to strong inward weakly sheared currents. One
372 notes also that, at each site, large value of vorticity can be observed during calm wind periods. The wave
373 effect is quite similar to that of the wind, although less marked. Strong wave events are generally related to
374 outward sheared currents at Isié and N'Digoro whereas at Tenia no clear dependency is observed.

375 From the data presented in Fig. 12 and an overall analysis of the measured profiles, the vertical structure
376 of the currents in passage and reef opening can be summarized as follows :

- 377 — During well-established currents and circulation patterns, the surface layers are generally moving
378 faster than the bottom ones.

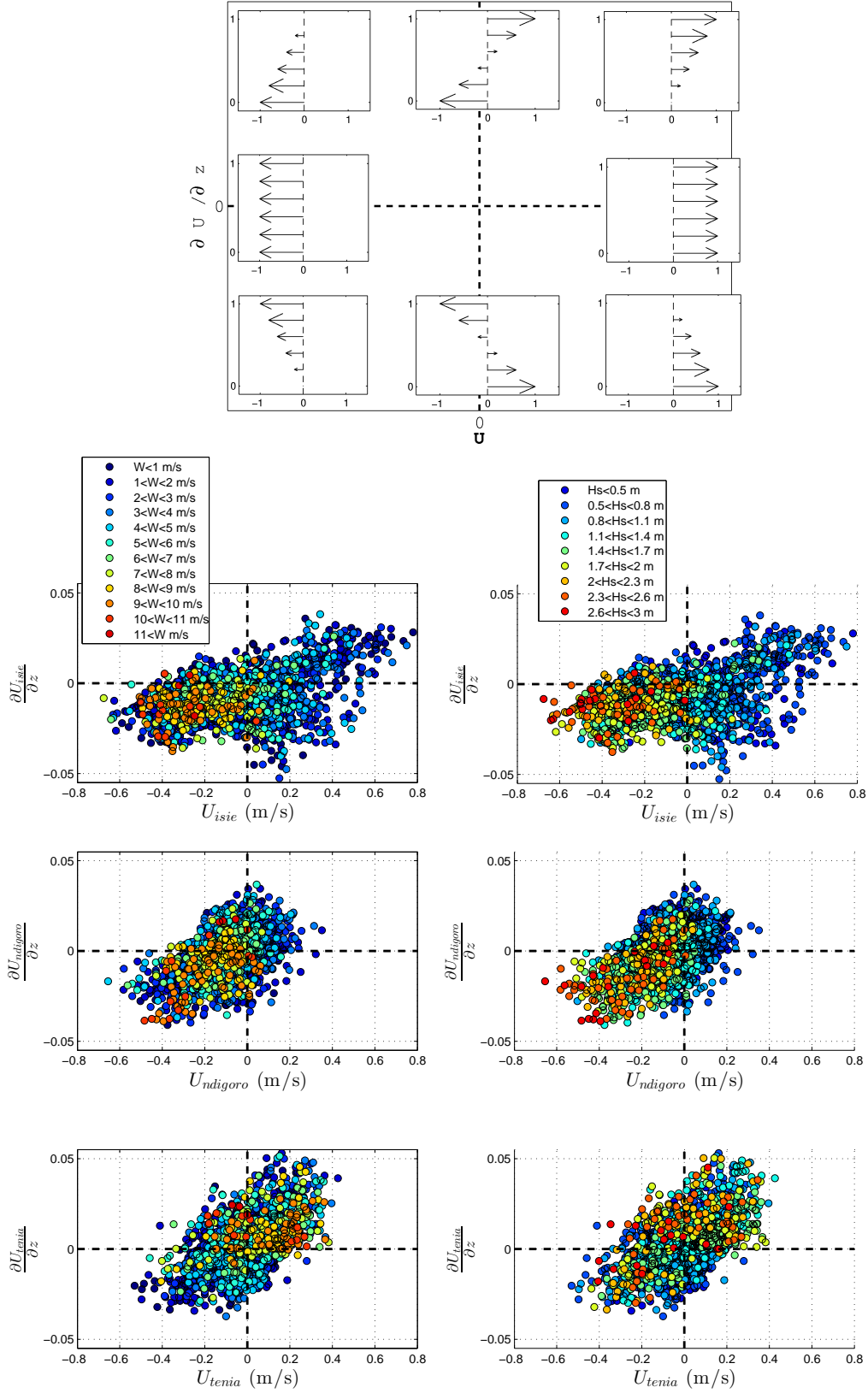


FIGURE 12: The top plot provides a scheme to help the data interpretation of the results in terms of vertical profiles, the x- and y-axis being the depth-averaged current and the vorticity, respectively. Current vorticity vs intensity for Isié, N'Digoro and Tenia. Color labels provide information of the wind magnitude (in m/s) and wave height (in m) for left and right plots, respectively.

379 — In most cases, the vorticity is roughly constant in the water column (linear velocity profile)
380 — The wind, generally eastern, affects as expected the vertical shear by accelerating the surface layer
381 when depth-averaged current is inward (e.g. during TRP events) or slowing down the surface layer of
382 outward flows.

383 — Opposite signs of depth-averaged velocity and vorticity can be observed, i.e. bottom layers moving
384 faster than surface ones, in particular (but not exclusively) during switchovers from TRP to CP.

385 Note that due to the time scales of the external forcings, in particular tide and thermal breeze, and
386 the lagoon depth (typically about 10m) and topographical constraints, the Ekman's effect on the current
387 vertical structure is expected to be weak, in particular in comparison to the direct action of wind stress at
388 the surface. Additional data processing will be carried out to further explore this issue.

389 4. Discussion

390 *A generic functioning for channel lagoons ?*

391 The hydrodynamical field measurements presented here provide a valuable dataset for the understanding
392 of lagoon circulation and a relevant benchmark for numerical modeling. It shows the importance of the
393 combined effects of tides, waves and wind which must all be taken into account in numerical models to
394 provide a proper characterization of water renewal dynamics. The main processes observed in the Ouano
395 lagoon should be representative of similar types of reef-lagoon systems that we defined as channel lagoons.
396 The distinctive features of such lagoons are :

- 397 — a well-defined barrier reef
- 398 — a typical lagoon depth (5-50m) much greater than the depth over the reef top (typically outcropping
399 during low spring tides),
- 400 — a reef-parallel dimension (length) of the lagoon much greater than the reef-normal dimension (width),
401 i.e. with an aspect ratio of the order of 2-10,
- 402 — longitudinal bathymetric gradients smaller than their transverse counterparts,
- 403 — one or several passages toward open ocean or adjacent lagoons.

404 Typical channel lagoons can be found for instance in the Pacific Ocean :

- 405 — New Caledonia, west and east coasts ;
- 406 — French Polynesia, east coast of Moorea, Huahiné, Raiatea-Tahaa, Tahiti Iti and Nui ;
- 407 — Japan, south-west Okinawa (Bibi beach) ;
- 408 — Fiji, Viti Levu, Nairai and Kandavu ;
- 409 — Samoa, Naunonga (Vanikoro), Utupoa ;

410 or in the Indian Ocean in Madagascar (Tulear) or in Maurice (north Mahebourg). Various tides, waves and
411 wind conditions can be encountered at each site but the renewal time of lagoon waters typically ranges from
412 few days to few weeks. Such time scales are, on one hand, sufficient to allow the setting up of a wide range of
413 bio-geochemical processes (the lagoon can produce its "own" waters) and, on the other hand, short enough
414 to be permanently affected by the fluctuations of ocean and atmospheric forcings : swell events, storms,
415 spring/neap tide cycles, winds, etc. The present experiments demonstrates that, in addition to the tidal
416 cycles, the wave and wind plays an important role in the lagoon circulation. The wave-breaking cross-reef
417 fluxes are generally able, independently to the tide, to renew the lagoon water in few days to few weeks. This wave

418 effect, which is enhanced as the length to width ratio of the lagoon increases, can drive different current
419 patterns depending on the swell direction and magnitude, possibly blocking or reversing the tidal fluxes
420 through passages and reef openings. The wind stress affects the vertical flow structure and also participate
421 to the reverse of the whole lagoon circulation when strongly blowing over a sufficient period of time (typically
422 few days). Depending on the lagoon geometry, the difference between patterns, which can alternatively drive
423 water from/into the open ocean or from/into the neighbouring lagoons in variable proportions, can lead to
424 important consequences in terms of water properties and biogeochemical processes.

425 *Seasonal variability*

426 The comparison between 2013 and 2015 experiments shows significant difference in occurrence probability
427 for CP and TRP (see Tab. 3), in relation with different wave and wind climates. The question arises on the
428 presence of a seasonal variation in the lagoon dynamics, with a dominant CP tendency during the austral
429 spring (August-November) and a dominant TRP tendency during the austral autumn (February-April).
430 This hypothesis is first supported by the preliminary experiment performed in 2011 from mid-july to october
431 which shows an dominant outward day-averaged flow at Ténia (about 67% of time), i.e. corresponding to CP
432 trend. Numerical wave statistics on the 1994-2012 period provided by WW3/IOWAGA data are depicted in
433 Fig. 13. The whole wave partitions are explored to compute the occurrence frequency of swells components
434 ($H_s > 1\text{m}$) coming from eastern ($\theta < 200^\circ$, black circles in Fig 13) and western ($\theta > 200^\circ$, red circles in Fig
435 13) sectors. A clear seasonal variation is observed : western swells are clearly dominant between may and
436 november while eastern swells are more present during the austral summer. In addition Meteo France wind
437 data at Tontouta airport from 2006 to 2015 are processed to depict the occurrence probability for strong
438 eastern winds ($W > 5\text{ m/s}$) in green circles in Fig. 13. A statistical trend is observed, with more frequent
439 strong wind events between September and March than during the rest of the year. According to the previous
440 analysis, it is likely that the difference in lagoon circulation observed between 2013 and 2015 (and 2011)
441 experiments are indeed representative of a cyclic seasonal variation. Even if the available hydrodynamical
442 data does not cover the full annual variations, one can expect a dominance of CP from may to september
443 when swells are predominantly from the west and winds are rather calm and, conversely, a dominant TRP
444 during the austral summer between December to April when strong winds and eastern swells are more
445 frequent. The renewal of lagoon waters should then be mainly controlled by inflow of open ocean waters
446 during the austral winter and inflow from south-eastern neighbouring lagoon through Tenia passage the rest
447 of the year.

448 *Impact of the Pam tropical cyclone*

449 Extreme meteorological events are able to strongly impact the flow pattern in reef-lagoon systems. This
450 is illustrated in the present dataset by the passage of the severe tropical cyclone Pam recorded during the
451 2015 experiments. The Pam tropical cyclone, which was one of the worst natural disasters in the history
452 of Vanuatu, formed on March 6, 2015 east of the Solomon Islands and moved southward when intensifying
453 to reach the Vanuatu islands on March 13 and finally decay on March 15 northeast of New Zealand. It is
454 responsible for the strong south to south-east winds (Tontouta airport measurements) and large waves (WW3
455 simulations) observed in between March 10 and 15. Such cyclone-related forcings induces the most intense
456 TRP conditions observed within the present dataset, with permanent strong inflow through Tenia passage

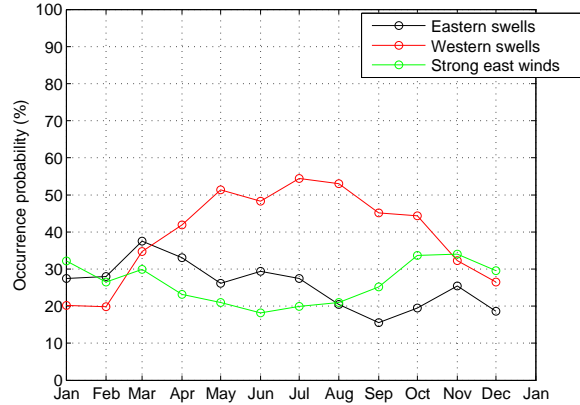


FIGURE 13: Occurrence probability of swells from eastern ($\theta < 200$, black circles in Fig 13) and western ($\theta > 200$, red circles in Fig 13) sectors from 1994-2012 IOWAGA/WW3 numerical datasets and strong eastern winds ($W > 5\text{m/s}$).

457 and outflow through the northern sites over more than 4 days which totally overcome the tidal dynamics
 458 (see Fig. 5). The clear regime shift from TRP to CP on March 14/15, while wave height and wind intensity
 459 remain strong, should probably be attributed to the slight shift in wind and waves directions. The proper
 460 validation of such an hypothesis would have require direct measurements of wave direction at the system
 461 entry, which are not available with the present dataset. However, this observation tends to highlight the
 462 increased sensitivity of the circulation system to the forcings direction during severe and extreme conditions.

463 *Biogeochemical issues*

464 The existence of well defined circulation patterns in the reef-lagoon system is of primary importance to
 465 analyse and predict the biological productivity and its evolution (Cuif et al., 2014). During CP conditions, the
 466 lagoon is mainly fueled by across-barrier water inputs. During the reef barrier crossing, coral organisms and
 467 plankton-eating fishes tend, through ingestion and metabolism, to modify the nutrient composition (uptake
 468 and regeneration), to deplete food content of the incoming waters by grazing and predation (bacterio-,
 469 phyto- and zooplankton content) (Houlbreque et al., 2006; Hamner and Hamner, 2000; Cuet et al., 2011)
 470 and to increase the release of non living particles (mucus) by corals (Cuet et al., 2011) . Furthermore, from
 471 the exchanged volumes estimated hereinbefore, one can expect that CP would be less efficient in terms of
 472 water renewal than TRP for which water are entering the lagon both through the Tenia passage and above
 473 the reef barrier. Longer residence times for CP may be associated with an increase of the phytoplanktonic
 474 productivity of the lagoon (Delesalle and Sournia, 1992; Andréfouët et al., 2001), which can compete with
 475 cross-reef transformation processes. TRP is expected to foster the inflow from neighbouring south-eastern
 476 lagoons through Tenia passage rather than open ocean waters. Visual observations notably revealed the
 477 arrival of water loaded with appendicularians and jellyfishes during TRP.

478 Current shearings generated by thermal and salinity fronts have been observed to induce strong plankton
 479 aggregation in the lagoon context (Gomez-Gutierrez et al., 2007). The present study demonstrates the
 480 presence of significant vertical shear induced by the wind forcing alone. The effect of such vertical shearing of
 481 the currents may significantly affect the plankton migration. For instance, in the passages and reef openings,
 482 a strongly sheared current with inflow at the surface and outflow near the bed (as revealed by the present

483 measurements) will play a dramatically different role depending on whether it occurs during day (zooplankton
484 lying near the bed) and during night (zooplankton close to the surface).

485 All of these open questions should drive further ambitious research efforts. In particular, field campaigns
486 must now be designed to measure *simultaneously* both hydrodynamical and biogeochemical properties of the
487 reef-lagoon systems in order to gain a comprehensive understanding of these coupled processes.

488 5. Conclusion

489 From two field campaigns carried out in the Ouano lagoon, west New Caledonia, we have identified the
490 main drivers of a typical channel lagoon. The selected lagoon - barrier reef system is exposed to south pacific
491 swells, meso-tides and trade winds modulated by the thermal breeze. A network of current profilers has
492 been deployed during two successive three-months field campaign in order to monitor the current within reef
493 passages and openings in a wide range of hydrodynamical and meteorological conditions. Pressure sensors
494 are used to monitor the incoming wave features on the outside reef slope.

495 The first driver of the lagoon hydrodynamics is the tide which induces periodic filling/flushing cycles
496 of the lagoon well identified on both free surface and currents measurements. In addition, a modulation of
497 currents at twice the tidal frequency has been observed, in response to the modulation of cross-reef flow
498 (Symonds et al., 1995; Kraines et al., 1998). The analysis of day-averaged depth-averaged currents allows to
499 identify both the inter-connections between measurement sites and their dependence to the external forcings.
500 The effect of wave is straightforward : as soon as waves break on the reef top, an entering flow is observed
501 above the reef barrier whatever the tide, increasing with wave energy. For the strongest swells, the cross-reef
502 water input is such as depth-averaged currents are permanently outward at each other site, even during rising
503 tide. For all other conditions, the current dynamics in reef openings and passages is mainly controlled by
504 wave direction and wind magnitude. The comparison between detided and day-averaged currents highlights
505 the slow day-scale adjustment of the lagoon circulation to the wind stress. Four typical circulations have
506 been characterized, with the two first controlling the lagoon dynamics more than 70% of time :

- 507 — The Classic Pattern corresponds to a day-averaged outflow at each passage and opening, occuring
508 during moderate wind and south-west wave conditions.
- 509 — The Tenia Reversal Pattern is defined by an input day-averaged flow at the southern opening driving
510 an overall bulk water motion toward north-west. This pattern is forced by strong winds and/or swells
511 coming from south-east
- 512 — The Isié and Southwards Patterns are observed in calm conditions. They are characterized by a reversal
513 of the day-averaged current in the northern opening of the lagoon. They are much less stable than
514 the two previous patterns which last for several days as long as the wave or wind forcings maintain.

515 Following the fluctuations of the meteorological forcings, the lagoon is expected to show a seasonal
516 functioning, with dominant inputs from open ocean waters and from neighbouring eastern lagoons during
517 austral summer and winter, respectively. Moreover, the sensitivity of the lagoon circulation to forcings
518 direction is expected to increase during severe and extreme wave and wind conditions encountered during
519 tropical storms or cyclones.

520 The analysis of the vertical structure of the current in lagoon passages shows the regular presence of
521 a significant nearly linear vertical shear in the water column. This shear often appears during strong wind
522 events but are also observed in calm conditions. The main tendency is that surface layer are faster than

523 bottom ones, either for in- or out-flows. Period of reversal between patterns are generally associated to
524 complex vertical structure of the current with opposite flows in the upper and lower parts of the water
525 column.

526 **Acknowledgements**

527 This study was sponsored by the Action Sud MIO/IRD (A.S. OLZO and A.S. CROSS-REEF) and the
528 ANR MORHOC'H (Grant No. ANR-13-ASTR-0007). The GLADYS group (www.gladys-littoral.org) sup-
529 ported the experimentation. We are grateful to all the contributors involved in this experiment. The authors
530 are particularly indebted to David Varillon, Eric Folcher and Bertrand Bourgeois whose efforts were essential
531 to the deployment. A special thanks is extended to Jérôme Aucan for giving immediate and unconditional
532 access to his data.

- 533 Andréfouët, S., Pages, J., Tartinville, B., 2001. Water renewal time for classification of atoll lagoons in the
534 tuamotu archipelago (french polynesia). *Coral reefs* 20 (4), 399–408.
- 535 Angwenyi, C. M., Rydberg, L., 2005. Wave-driven circulation across the coral reef at bamburi lagoon, kenya.
536 *Estuarine, Coastal and Shelf Science* 63 (3), 447–454.
- 537 Atkinson, M., Smith, S., Stroup, E., 1981. Circulation in enewetak atoll lagoon. *Limnol Oceanogr* 26 (6),
538 1074–1083.
- 539 Bonneton, P., Lefebvre, J.-P., Bretel, P., Ouillon, S., Douillet, P., 2007. Tidal modulation of wave-setup and
540 wave-induced currents on the aboré coral reef, new caledonia. *J. Coast. Res* 50, 762–766.
- 541 Carassou, L., Le Borgne, R., Rolland, E., Ponton, D., 2010. Spatial and temporal distribution of zooplankton
542 related to the environmental conditions in the coral reef lagoon of new caledonia, southwest pacific. *Marine
543 pollution bulletin* 61 (7), 367–374.
- 544 Chevalier, C., Devenon, J.-L., Rougier, G., Blanchot, J., 2014. Hydrodynamics of the toliara reef lagoon
545 (madagascar) : Example of a lagoon influenced by both waves and tide. *Journal of Coastal Research*.
- 546 Chevalier, C., Sous, D., Devenon, J.-L., Pagano, M., Rougier, G., Blanchot, J., 2015. Impact of cross-reef
547 water fluxes on lagoon dynamics : a simple parameterization for coral lagoon circulation model, with
548 application to the ouano lagoon, new caledonia. *Ocean Dynamics* 65 (11), 1509–1534.
- 549 Cuet, P., Atkinson, M., Blanchot, J., Casareto, B., Cordier, E., Falter, J., Frouin, P., Fujimura, H., Pierret,
550 C., Susuki, Y., et al., 2011. Cnp budgets of a coral-dominated fringing reef at la réunion, france : coupling
551 of oceanic phosphate and groundwater nitrate. *Coral Reefs* 30 (1), 45–55.
- 552 Cuif, M., Kaplan, D. M., Lefèvre, J., Faure, V. M., Caillaud, M., Verley, P., Vigliola, L., Lett, C., 2014.
553 Wind-induced variability in larval retention in a coral reef system : A biophysical modelling study in the
554 south-west lagoon of new caledonia. *Progress in Oceanography* 122, 105–115.
- 555 Delesalle, B., Sournia, A., 1992. Residence time of water and phytoplankton biomass in coral reef lagoons.
556 *Continental Shelf Research* 12 (7), 939–949.
- 557 Delhez, E. J., Campin, J.-M., Hirst, A. C., Deleersnijder, E., 1999. Toward a general theory of the age in
558 ocean modelling. *Ocean Modelling* 1 (1), 17–27.
- 559 Delhez, É. J., de Brye, B., de Brauwere, A., Deleersnijder, É., 2014. Residence time vs influence time. *Journal
560 of Marine Systems* 132, 185–195.
- 561 Fernando, H., McCulley, J., Mendis, S., Perera, K., 2005. Coral poaching worsens tsunami destruction in sri
562 lanka. *Eos, Transactions American Geophysical Union* 86 (33), 301–304.
- 563 Gomez-Gutierrez, J., Martínez-Gómez, S., Robinson, C. J., 2007. Influence of thermo-haline fronts forced
564 by tides on near-surface zooplankton aggregation and community structure in bahía magdalena, mexico.
565 *Marine Ecology Progress Series* 346, 109–125.
- 566 Gourlay, M., 1996a. Wave set-up on coral reefs. 1. set-up and wave-generated flow on an idealised two
567 dimensional horizontal reef. *Coastal Engineering* 27 (3), 161–193.

- 568 Gourlay, M., 1996b. Wave set-up on coral reefs. 2. set-up on reefs with various profiles. *Coastal Engineering*
569 28 (1), 17–55.
- 570 Gourlay, M. R., Colleter, G., 2005. Wave-generated flow on coral reefs—an analysis for two-dimensional
571 horizontal reef-tops with steep faces. *Coastal Engineering* 52 (4), 353–387.
- 572 GRENZ, C., Le Borgne, R., Torreton, J.-P., FICHEZ, R., 2013. New caledonia lagoon : a threatened paradise
573 under anthropogenic pressure? *Lagoons : Habitat and Species, Human Impacts and Ecological Effects*,
574 xx–xx.
- 575 Hamner, W. M., Hamner, P. P., 2000. Behavior of antarctic krill (*euphausia superba*) : schooling, foraging,
576 and antipredatory behavior. *Canadian Journal of Fisheries and Aquatic Sciences* 57 (S3), 192–202.
- 577 Hardy, T. A., Young, I. R., 1996. Field study of wave attenuation on an offshore coral reef. *Journal of*
578 *Geophysical Research : Oceans* (1978–2012) 101 (C6), 14311–14326.
- 579 Hearn, C., Parker, I., 1988. Hydrodynamic processes on the ningaloo coral reef, western australia. In :
580 *Proceedings of the Sixth International Coral Reef Symposium. Vol. 2.* pp. 497–502.
- 581 Hearn, C. J., 1999. Wave-breaking hydrodynamics within coral reef systems and the effect of changing relative
582 sea level. *Journal of Geophysical Research : Oceans* (1978–2012) 104 (C12), 30007–30019.
- 583 Hench, J. L., Leichter, J. J., Monismith, S. G., 2008. Episodic circulation and exchange in a wave-driven
584 coral reef and lagoon system. *Limnology and Oceanography* 53 (6), 2681.
- 585 Hoeke, R. K., Storlazzi, C. D., Ridd, P. V., 2013. Drivers of circulation in a fringing coral reef embayment : a
586 wave-flow coupled numerical modeling study of hanalei bay, hawaii. *Continental Shelf Research* 58, 79–95.
- 587 Houlbreque, F., Delesalle, B., Blanchot, J., Montel, Y., Ferrier-Pagès, C., et al., 2006. Picoplankton removal
588 by the coral reef community of la prévoyante, mayotte island. *Aquatic microbial ecology* 44, 59–70.
- 589 Kench, P., McLean, R., 2004. Hydrodynamics and sediment flux of hoa in an indian ocean atoll. *Earth*
590 *Surface Processes and Landforms* 29 (8), 933–953.
- 591 Kraines, S., Yanagi, T., Isobe, M., Komiyama, H., 1998. Wind-wave driven circulation on the coral reef at
592 bora bay, miyako island. *Coral Reefs* 17 (2), 133–143.
- 593 Kraines, S. B., Suzuki, A., Yanagi, T., Isobe, M., Guo, X., Komiyama, H., 1999. Rapid water exchange
594 between the lagoon and the open ocean at majuro atoll due to wind, waves, and tide. *Journal of Geophysical*
595 *Research : Oceans* (1978–2012) 104 (C7), 15635–15653.
- 596 Lowe, R. J., Falter, J. L., Bandet, M. D., Pawlak, G., Atkinson, M. J., Monismith, S. G., Koseff, J. R.,
597 2005. Spectral wave dissipation over a barrier reef. *Journal of Geophysical Research : Oceans* (1978–2012)
598 110 (C4).
- 599 Lowe, R. J., Falter, J. L., Monismith, S. G., Atkinson, M. J., 2009. Wave-driven circulation of a coastal
600 reef-lagoon system. *Journal of Physical Oceanography* 39 (4), 873–893.

- 601 Lugo-Fernandez, A., Roberts, H., Wiseman Jr, W., 1998. Tide effects on wave attenuation and wave set-up
602 on a caribbean coral reef. *Estuarine, Coastal and Shelf Science* 47 (4), 385–393.
- 603 Massel, S., Gourlay, M., 2000. On the modelling of wave breaking and set-up on coral reefs. *Coastal Engi-*
604 *neering* 39 (1), 1–27.
- 605 Masselink, G., 1998. Field investigation of wave propagation over a bar and the consequent generation of
606 secondary waves. *Coastal Engineering* 33 (1), 1–9.
- 607 Monismith, S. G., 2007. Hydrodynamics of coral reefs. *Annu. Rev. Fluid Mech.* 39, 37–55.
- 608 Monsen, N. E., Cloern, J. E., Lucas, L. V., Monismith, S. G., 2002. A comment on the use of flushing time,
609 residence time, and age as transport time scales. *Limnology and Oceanography* 47 (5), 1545–1553.
- 610 Pomeroy, A., Lowe, R., Symonds, G., Van Dongeren, A., Moore, C., 2012. The dynamics of infragravity wave
611 transformation over a fringing reef. *Journal of Geophysical Research : Oceans* (1978–2012) 117 (C11).
- 612 Roberts, H. H., Murray, S. P., Suhayda, J. N., 1975. Physical processes in fringing reef system. *Journal of*
613 *Marine Research* 33 (2), 233–260.
- 614 Roberts, H. H., Suhayda, J. N., 1983. Wave-current interactions on a shallow reef (nicaragua, central america).
615 *Coral Reefs* 1 (4), 209–214.
- 616 Symonds, G., Black, K. P., Young, I. R., 1995. Wave-driven flow over shallow reefs. *Journal of Geophysical*
617 *Research : Oceans* (1978–2012) 100 (C2), 2639–2648.
- 618 Szmant, A. M., 2002. Nutrient enrichment on coral reefs : is it a major cause of coral reef decline ? *Estuaries*
619 25 (4), 743–766.
- 620 Taebi, S., Lowe, R. J., Pattiaratchi, C. B., Ivey, G. N., Symonds, G., Brinkman, R., 2011. Nearshore circu-
621 lation in a tropical fringing reef system. *Journal of Geophysical Research : Oceans* (1978–2012) 116 (C2).
- 622 Tartinville, B., Rancher, J., 2000. Wave-induced flow over mururoa atoll reef. *Journal of Coastal Research*,
623 776–781.
- 624 Van Dongeren, A., Lowe, R., Pomeroy, A., Trang, D. M., Roelvink, D., Symonds, G., Ranasinghe, R., 2013.
625 Numerical modeling of low-frequency wave dynamics over a fringing coral reef. *Coastal Engineering* 73,
626 178–190.
- 627 Wolanski, E., Delesalle, B., Dufour, V., Aubanel, A., et al., 1993. Modeling the fate of pollutants in the tiahura
628 lagoon, moorea, french polynesia. In : 11th Australasian Conference on Coastal and Ocean Engineering :
629 Coastal Engineering a Partnership with Nature ; Preprints of Papers. Institution of Engineers, Australia,
630 p. 583.